SEMARAK ILMU PUBLISHING

Semarak Engineering Journal

Journal homepage:
https://semarakilmu.my/index.php/sej/index
ISSN: 3036-0145

Parametric Study of Foam-filled Trapezoidal Sandwich Beam

Liew Se Hau[1], Yulfian Aminanda[1,*]

[1] Universiti Teknologi Brunei, Jalan Tungku Link Gadong, BE1410 Brunei Darussalam

ARTICLE INFO

Article history:
Received 15 August 2025
Received in revise 16 September 2025
Accepted 25 September 2025
Available online 22 December 2025

Keywords:
Trapezoidal corrugated; composite; finite element analysis; quasi-static compression; foam; energy absorption

ABSTRACT

Foam-filled trapezoidal sandwich structure provides high stiffness-to-weight ratio. There exists limited research on identifying the best configuration through parametric study but instead were focused on creating novel structures. The aim is to employ numerical approach through finite element analysis (FEA) to establish the key parameters which includes the core geometry, core material, fibre orientation, ply thickness, foam-filling, and foam density under quasi-static compression. The change from aluminium core to woven CFRP core with [0°/0°/0°/0°] layup increases the peak load and specific energy absorption (SEA) to 62.4 kN and 7.76 kJ/kg respectively. A ply thickness of 2.5 mm provides the highest SEA of 20 kJ/kg when measured at 80% peak load. The 90° corrugation angle exhibits SEA of 11.16 kJ/kg at 4 mm displacement which is approximately double that of 45° angle. The best core height is 9.85 mm associated with SEA of 8.55 kJ/kg compared to increased heights. Foam-filling with aluminium foam of density 500 kg/m^3 increases SEA by 36.68%, 32.82%, and 121.37% when compared to summation of pure foam and empty corrugated core, pure foam core, and empty corrugated core respectively, which switching to a foam density of 1100 kg/m^3 yields a SEA of 9.62 kJ/kg, an 85.71% increase.

1. Introduction

Sandwich structures are composed of a central core bonded between two face sheets which provides for enhanced mechanical properties in high stiffness-to-weight ratio applications. Amongst the many core configuration available, corrugated core have gained popularity due to its enhanced strength combined with open cell ventilation benefit to prevent moisture retention [1, 2, 3]. There are much researches conducted on improving the performance of trapezoidal core through several key parameters. This can be through varying the geometry, which the effect of increasing core thickness and decreasing core height enhances the elastic and shear moduli, compressive strength, and SEA [4,5]. Additionally, an increase in corrugation angle raises the elastic modulus, compressive strength, and energy absorption capabilities [6,7].

[1*] *Corresponding author.*
E-mail address: yulfian.aminanda@utb.edu.bn

https://doi.org/10.37934/sej.10.1.6575

There also exist a large variety of material that can be applied to the core. Previously, metallic core was commonly used, Biagi *et al*., [8] investigated the in-plane compression response of aluminium corrugated core, but in recent applications, composite materials are often the preferred material to construct the core as it is known to enhance performance at a lighter weight, which prompted study of different methods to further enhance composite materials such as CFRP through varying fibre orientations [9,10].

The benefits of foam-filling the interstitial voids between the corrugated core have been demonstrated by studies to show increase compressive strength and SEA compared to empty corrugated core, pure foam core, and the summation of the two [11-13]. Additionally, the density of the foam used in foam-filling affects the mechanical properties of the entire structure, where Han *et al.*, [14] showed doubling the density of the foam will increase the SEA by approximately two times.

Recent studies focuses on the advancement of sandwich structures through developing novel sandwich structures such as multi-layered sandwich panels with varying stacking sequence [15, 16] or bi-directional corrugated sandwich structures [17], leaving a significant knowledge gap in the area of parametric optimisation of the already existing trapezoidal sandwich structure, which limits its overall mechanical capabilities which may be sufficient to achieve the functional requirement of a specific application without introducing novel configurations that will potentially incur more cost and complexity.

The key parameters identified that affects the SEA performance were the core geometry (angle and height), core thickness (ply thickness for composites), composite fibre orientation, addition of foam-filling, and foam densities. This presents a ground for further parametric study to determine the best configuration for a trapezoidal sandwich panel under quasi-static compression using numerical approach. This includes developing a validated numerical model as a basis for conducting parametric study and defining a design chart that will aid in optimising the mechanical performance to the weight for different applications.

2. Methodology

2.1 Validation model

The large number of parametric changes required in this study calls for the use of commercial FEA simulation software. This effectively reduces the cost and time required for fabrication of experimental specimens. The finite element model (FEM) was developed in ANSYS Workbench to undergo quasi-static compression. The validation model was constructed based on the experimental and numerical work of Rong *et al*., [18], which the material properties and core geometry can be found, the face sheet material is an unidirectional CFRP [0°/90°/0°/90°] stacking sequence with dimensions of 96 mm x 96 mm x 1 mm and with corrugated core material being aluminium alloy and having core angle = 55°, core height = 12.85 mm, core thickness = 0.5 mm, and length of unit cell = 32 mm. Both the core and face sheets were created using shell elements in ANSYS Workbench for computational efficiency. A mesh size of 2.5 mm was applied to the face sheets and the core and the contact definition were set as bonded which prevents delamination.

Under the analysis settings, end time of 0.3 s and enhanced composite damage model was utilized for composite failure, with the rest program controlled. A displacement boundary condition was applied to the top surface of the top face sheet at -5.0 mm in the Z-component while restricted in X and Y components. A fixed support boundary condition was applied to the bottom of the bottom face sheet. The load was measured as the reaction force on the bottom of the bottom face sheet and internal energy was taken for the whole assembly.

The validation process was carried out by comparing the important characteristics such as the peak load and deformation behaviour observed in the force-displacement graph. The percentage error between the peak load falls within 5.2% showing good agreement between numerical and experimental results for further parametric study. The ANSYS 3D model is as shown in Figure 1 with indication of the loading and boundary conditions.

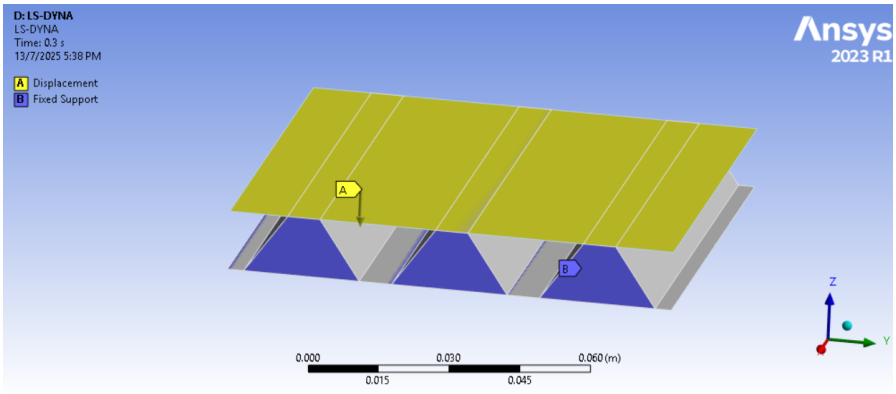

Fig. 1. Loading and boundary condition for sandwich structure

2.2 Parametric Study Setup

The actual model was constructed following the procedures in the validation model, with the only variations being swapping of material between face sheets (to aluminium) and core (to woven CFRP), the unidirectional CFRP laminate were also changed to woven CFRP laminate to enhance performance, and Flanagan-Belytschko Viscous Form with hourglass coefficient = 0.1 was applied under analysis setting. Tsai-Wu Failure Criterion [19] was applied to the CFRP core as the failure model for orthotropic materials which combines tensile and compressive strengths into a single equation, and failure occurs when the following equation yields to more than 1:

$$F_i\sigma_i + F_{ij}\sigma_i\sigma_j \geq 1 \qquad (1)$$

Where σ_i, σ_i = stress components and F_i, F_{ij} = strength tensors derived from material strength

The orthotropic properties for woven CFRP laminate applied to the core were as default in the ANSYS Engineering Data library, where detailed listing can be found in Table 1 to Table 3.

Table 1
Orthotropic elasticity of woven CFRP

Properties	*Value*
Longitudinal stiffness, E_{11}	91.82 GPa
Transverse stiffness, E_{22}	91.82 GPa
Out-of-plane stiffness, E_{33}	9 GPa
Poisson's ratio, v_{12}	0.05
Poisson's ratio, v_{13}, v_{23}	0.3
Shear modulus, G_{12}	3.6 GPa
Shear modulus, G_{23}, G_{13}	3 GPa
Density, ρ	1480 kg/m^3

Table 2
Orthotropic stress limit of woven CFRP

Properties	*Value*
Tensile X direction	829 MPa
Compressive X direction	-439 MPa
Tensile Y direction	829 MPa
Compressive Y direction	-439 MPa
Tensile Z direction	50 MPa
Compressive Z direction	-140 MPa
Shear XY	120 MPa
Shear YZ	50 MPa

Table 3
Orthotropic strain limit of woven CFRP

Properties	*Value*
Tensile X direction	0.0086
Tensile Y direction	0.0086
Tensile Z direction	0.007
Compressive X direction	-0.0055
Compressive Y direction	-0.0055
Compressive Z direction	-0.012
Shear XY	0.022
Shear YZ	0.018

The material comparison (aluminium core with woven CFRP core) was carried out, followed by variation in fibre orientation, corrugation ply thickness, angle, and height. This leads to the addition of foam-filling, where the foam materials were modelled as solid elements using the crushable foam material model to feature non-linear compressive characteristics. Table 4 list the foam densities with its mechanical properties that were calculated based on given foam properties by Han et al. [14] as there was a lack of literature data on the mechanical properties on aluminium foam, which measures were taken to interpolate the stress-strain graph of the existing graph to obtain new curves for different densities and applying scaling law for Young's Modulus of cellular material by Gibson and Ashby [20] given by

$$\frac{E}{E_s} = C\left(\frac{\rho}{\rho_s}\right)^n \quad (2)$$

where E = Young's Modulus of the new foam, E_s = Young's Modulus of the parent foam, ρ = Density of the new foam, ρ_s = Density of the parent foam, C and n are constants which C = 1 and n = 2 are conventionally adopted.

Table 4
Mechanical properties of different aluminium foam densities

Foam Densities (kg/m^3)	*Elastic Modulus (GPa)*
500	1.546
648	2.61
800	5.27
900	10.07
1000	15.53
1100	22.97

The previous boundary conditions, meshing, contact definition, and analysis setting were kept constant, with a change in face sheet geometry into 96 mm x 32 mm x 1 mm and the core from three-unit cell to one, and thickness of 0.25 mm for computational efficiency. Additional contact definition was set between the foam to the face sheets and core, which is applied as perfectly bonded as per Yan *et al*., [11], it captures the deformation better in the early-stage deformation. Mesh size of 2.5 mm was also applied.

2.3 Parametric Configurations

The fibre orientation to be studied are: [0°/0°/0°/0°], [45°/45°/45°/45°], [0°/45°/0°/45°], [0°/0°/45°/45°], [45°/0°/0°/45°], [0°/45°/45°/0°], and [45°/45°/0°/0°]. As for the ply thickness, the configurations chosen are: 4-ply, 8-ply, 12-ply, 16-ply, 20-ply, and 24-ply. For the geometry, it includes the corrugation angle and height which are: 45°, 55°, 65°, 75°, 90° and 9.85 mm, 10.85 mm, 12.85 mm, 14.85 mm, 16.85 mm respectively. For foam-filling, initially foam density of 500 kg/m^3 was used to determine the effects of foam-filling, and later varying foam densities were applied: 648 kg/m^3, 800 kg/m^3, 900 kg/m^3, 1000 kg/m^3, and 1100 kg/m^3..

The peak load is the maximum force observable during the simulation process whereas SEA is the energy absorption per unit mass, which is a much more effective way of comparing different parameters when there is change in mass, such as different ply thickness and foam densities. The energy absorption and SEA is given by

$$Energy\ Absorption, EA = \int_0^{\delta} f(x)dx \quad (3)$$

$$Specific\ Energy\ Absorption, SEA = \frac{EA}{m} \quad (3)$$

where δ = displacement at a certain chosen point (mm), f(x) = load or reaction force observed by reference point node (kN), x = displacement, (mm), m = mass of the sandwich structure (kg)

3. Results

3.1 Variation in Fibre Orientation

The force-displacement curves for different fibre orientations are shown in Figure 2, which highlights a similar graphical characteristic, starting off with an initial linear rise to a peak load and gradually decreasing into a plateau before reaching densification. The [0°/0°/0°/0°] layup achieves a highest peak load of 62.4 kN, while the [45°/45°/45°/45°] layup is the lowest at 41.6 kN as per Figure 3. The potential reason for the difference may be attributed to the fibre direction aligning with the load path at a [0°/0°/0°/0°] layup as the inclined wall undergoes axial and shear stresses as opposed

to a [45°/45°/45°/45°] layup, thus leading to earlier failure such as buckling or matrix cracking due to more burden on the polymer matrix.

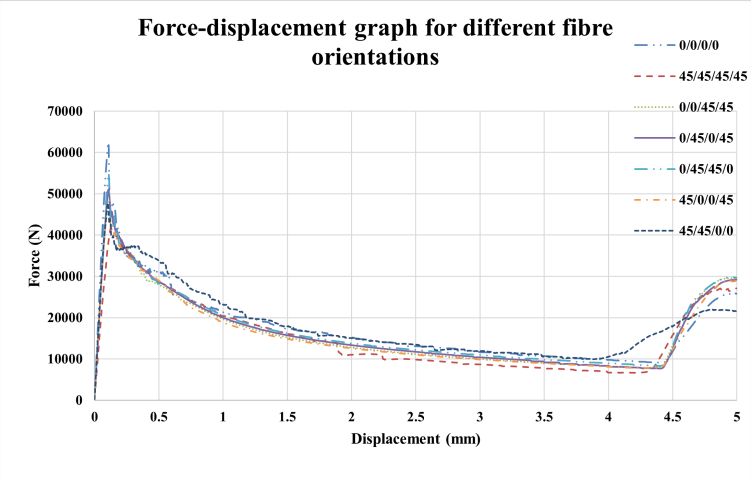

Fig. 2. Force-displacement graph for different fibre orientations

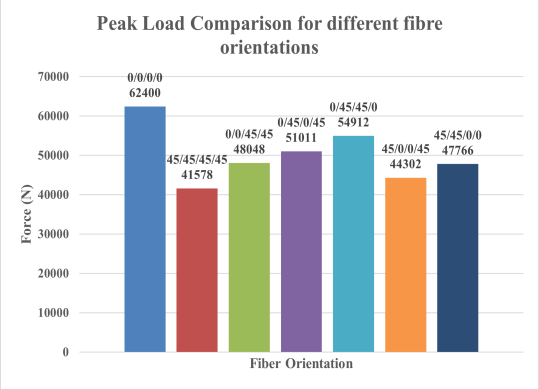

Fig. 3. Chart of peak load comparison for different fibre orientations

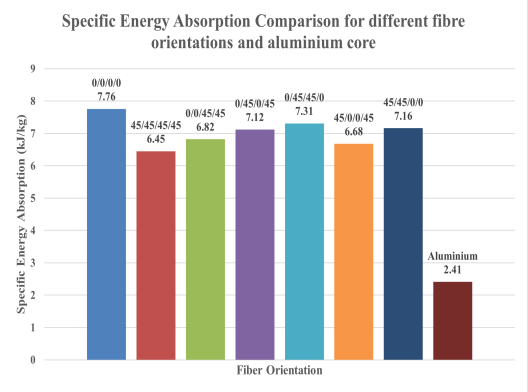

Fig. 4. Chart of SEA comparison for different fibre orientations

SEA characteristics of different fibre orientations are shown in Figure 4, due to higher peak load and plateau load for [0°/0°/0°/0°] layup, the highest SEA was also achieved of 7.76 kJ/kg, 20.31% increase from [45°/45°/45°/45°] layup with lowest SEA of 6.45 kJ/kg. Comparison was also made between aluminium core and woven CFRP, where [0°/0°/0°/0°] layup shows substantial improvement by 222.41% when switching to woven CFRP core.

3.2 Variation in Fibre Ply Thickness

The different ply configurations applied are compared using the force-displacement curve in Figure 5, where an increase in thickness results in a higher peak load but with a more gradual decrease in load instead of sharp drop compared to lower thickness. The 24-ply configuration has the highest peak load which can be attributed to the bulk of material available to resist deformation. The more gradual load decrease is caused by progressive failure rather than instant buckling that will be

caused by a lower number of plies. Figure 6 shows the chart of SEA between different ply-configurations, which at a displacement of 5 mm, the 20-ply configuration have the highest SEA of 28.19 kJ/kg as compared to the lowest which is the 4-ply configuration with 8.85 kJ/kg, which is an improvement of 218.53%. It is also to note that the 12-ply configuration have a higher initial SEA as compared to the rest up to a displacement of 2 mm which may be useful for early-stage energy absorption applications. Further increasing the ply above 20 plies will result in a lower SEA due to the weight as per Figure 6.

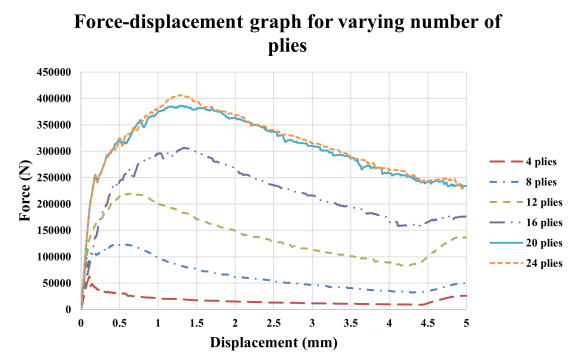

Fig. 5. Chart of peak load comparison for different number of plies

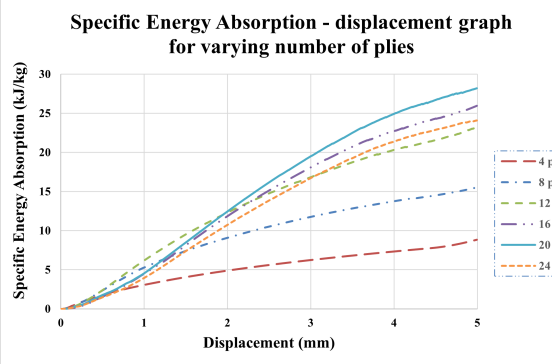

Fig. 6. Chart of SEA comparison for different number of plies

Figure 7 shows the SEA at peak load which can be useful for early-stage deformation that requires lightweight and high early-stage SEA. In this case, 16-ply configuration has the best SEA at 6.94 kJ/kg and lowest SEA at 4-ply with 0.27 kJ/kg. As for Figure 8, the chart shows the different SEA at 80% peak load, which is conveniently adopted, showing that 20-ply configuration have the highest SEA at 20.00 kJ/kg as compared to the lowest of 4-ply at 0.32 kJ/kg. Further increase in plies beyond 20-ply will not have a further increase in SEA. The choice of selecting the ply configuration depends on whether lightweight design with early-stage SEA is desired, which a 16-ply configuration will be the best. However, if crashworthy design is the priority, higher SEA across a longer displacement is essential, which the 20-ply configuration will be chosen.

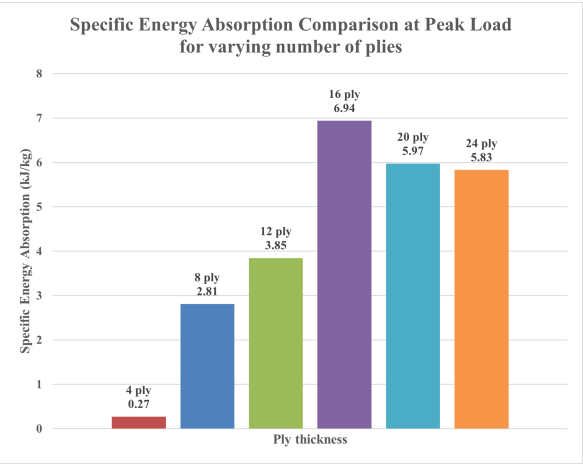

Fig. 7. Chart of SEA at peak load for varying number of plies

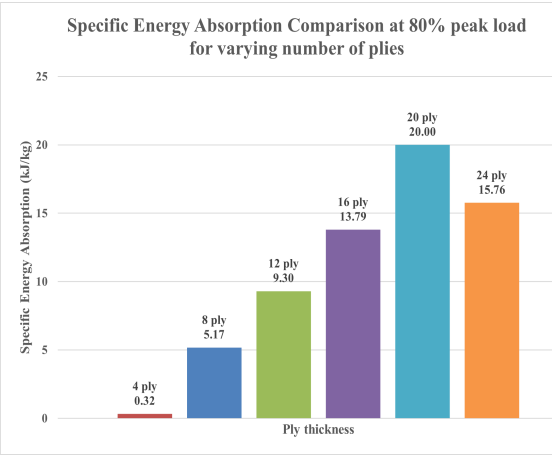

Fig. 8. Chart of SEA comparison for at 80% peak load for varying number of plies

3.3 Variation in Corrugation Angle and Core Height

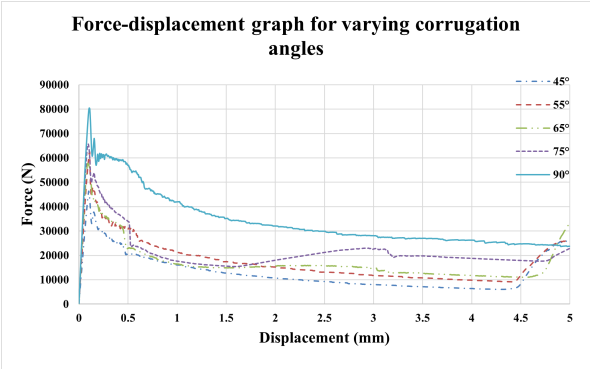

Fig. 9. Force-displacement graph for varying corrugation angles

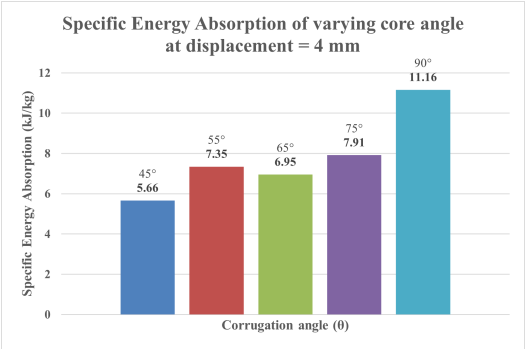

Fig. 10. Chart of SEA comparison for different corrugation angles

Figure 9 shows the force-displacement graph for varying corrugation angles, where an increase in corrugation angle leads to increase in load carrying capacity. A 90° corrugation angle exhibits the highest peak load of 80.4 kN and following plateau load, which is compared to the 45° corrugation angle with peak load of 46.3 kN. The reason may be attributed to the load path aligning with the fiber direction as it moves toward the 90° configuration, thus usually only axial stress applies to the core for the 90° configuration, whereas the 45° have induced shear stresses that will cause earlier failure. Similarly, due to the higher peak load and plateau load, the 90° configuration corresponds to a higher SEA of 11.16 kJ/kg which is an increase of 97.17% from 45° angle as per Figure 10.

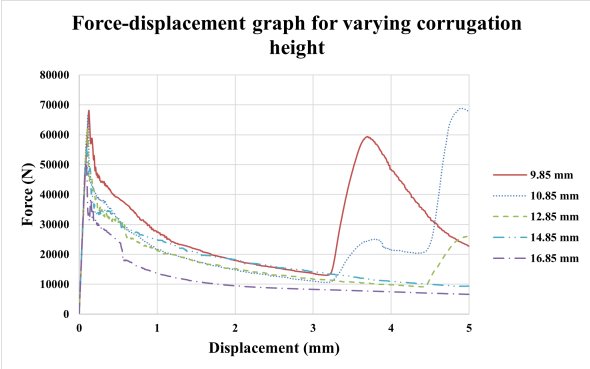

Fig. 11. Force-displacement graph for varying corrugation heights

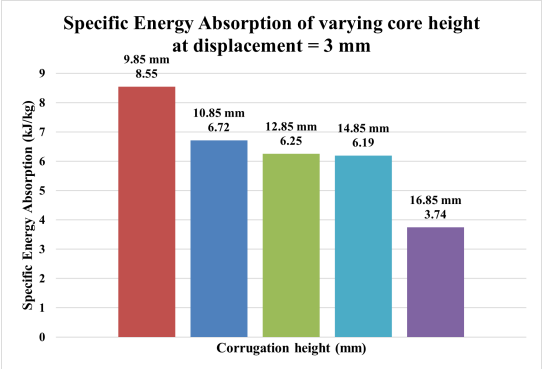

Fig. 12. Chart of SEA comparison for different corrugation heights

Figure 11 shows the peak load characteristics of the different corrugation height, which the 16.85 mm taller core have a lower peak load at 50.1 kN and it increases to peak load of 68.1 kN when corrugation height of 9.85 mm is applied, which is a 36.0% increase in peak load, but as observed it reaches densification earlier, thus can only absorb energy at a shorter range of displacement. The SEA of different corrugation height is compared in Figure 12, where a decreasing core height corresponds to a higher SEA at earlier stages of displacement up to 3 mm. The 9.85 mm core height have a 128.6% increase in SEA from a core height of 16.85 mm. The reason being that the taller height will lead to easier buckling of the core.

3.4 Effect of Foam-Filling and Varying Foam Densities

Figure 13 shows the force-displacement graph for different configurations of foam-filling, where the foam-filled core has the highest peak load and corresponding plateau load. This is greater than that of empty core, pure foam core, and summation of foam core and empty core. SEA comparison was shown in Figure 14, where the foam-filled sandwich structure has 5.18 kJ/kg SEA, which is an increase of SEA by 36.68%, 32.82%, and 121.37% when compared to summation of pure foam and empty corrugated core, pure foam core, and empty corrugated core respectively. This shows that the foam-filling does not act as a summation of the two combined, but instead there are positive mechanical interactions between them, where the foam provides bulk and the core restricts deformation.

Figure 15 shows the force-displacement curve of varying density up to a strain of 0.3, where an increase in foam density raises the peak and plateau forces due to higher density correlates to higher stiffness and compressive strength. The 1100 kg/m^3 foam exhibits highest peak and plateau load which relating to Figure 16, produces the highest SEA of 9.62 kJ/kg, while the lowest density of 500 kg/m^3 exhibits SEA of 5.18 kJ/kg, which is an 85.71% difference from lowest to highest foam density. The higher SEA associated with density of 1100 kg/m^3 does not mean there is no use of lower density foam, as certain applications require lighter weight and do not require a high SEA which is not achievable with the higher density.

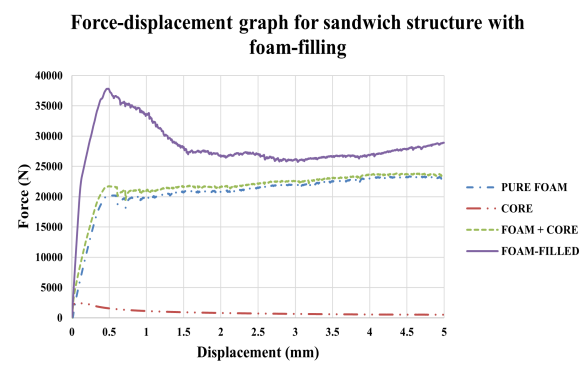

Fig. 13. Force-displacement graph for sandwich structure with foam-filling

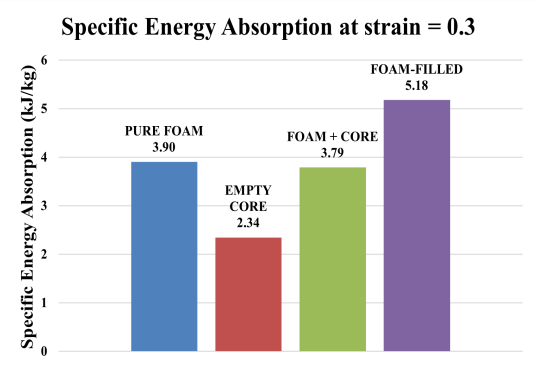

Fig. 14. Chart of SEA comparison for sandwich structure with foam-filling

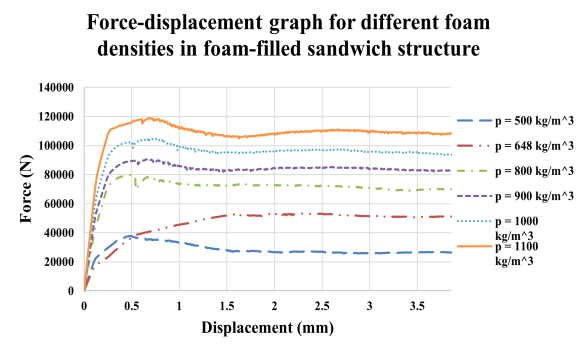

Fig. 15. Force-displacement graph for sandwich structure with varying densities

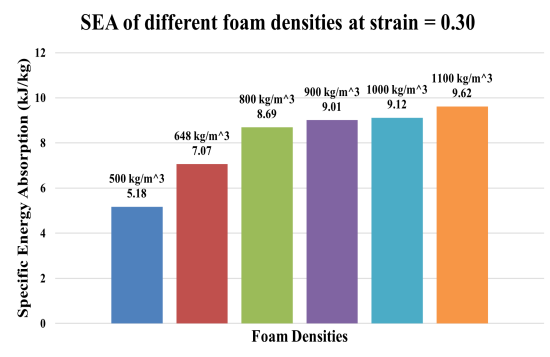

Fig. 16. Chart of SEA comparison for varying densities at strain = 0.30

4. Conclusion

This study has presented a comprehensive numerical approach to conduct a parametric investigation on trapezoidal sandwich structures to determine the best design configuration to enhance the overall performance when subjected to quasi-static compression. The aim of filling the research gap of determining the best configuration to maximize the overall performance of trapezoidal sandwich structures was addressed through the choice of material, variation in core geometry, fiber orientation and thickness, effect of foam-filling and the respective variation in the foam densities.

The first variation includes changing to a woven CFRP core from an aluminium core, which have a higher SEA with the same thickness with peak load of 62.4 kN. This is an increase from a SEA of 2.41 kJ/kg by the aluminium core to a SEA of 7.76 kJ/kg by the CFRP core, a 222.41% rise in SEA. The CFRP with [0°/0°/0°/0°] layup is the best fibre orientation due to the alignment of the fibre with the load path in the inclined walls of the core, which is 20.31% increase from [45°/45°/45°/45°] layup which shear stresses are induced. A 20-ply configuration have the best overall SEA of 28.19 kJ/kg, a 218.53% increase from 4-ply configuration at 8.85 kJ/kg. The excellent performance is due to increased bulk of material. 90° corrugation angle exhibits the highest peak load of 80436 N and an increase of 97.17% as the corrugation angle changes from 45° with SEA of 5.66 kJ/kg to a SEA of 11.16 kJ/kg when subjected to quasi-static loading due to the fibre directions aligning with the load path. The SEA of core height 9.85 mm is 8.55 kJ/kg, whereas the 16.85 mm corrugation height exhibits a lowest SEA of 3.74 kJ/kg. Foam-filling with aluminium foam of density of 500 kg/m^3 produces a SEA of 5.18 kJ/kg which is an increase by 36.68%, 32.82%, and a 121.37% when compared to summation of pure foam core and empty corrugated core, pure foam core, empty corrugated core respectively. Foam density of 1100 kg/m^3 corresponds to SEA of 9.62 kJ/kg while density of 500 kg/m^3 corresponds to 5.18 kJ/kg, which is an 85.71% increase in SEA, and highest among all the densities that were tested.

Acknowledgement

This research was not funded by any grant.

References

[1] Ma, Quanjin, M. R. M. Rejab, J. P. Siregar, and Zhongwei Guan. "A review of the recent trends on core structures and impact response of sandwich panels." *Journal of Composite Materials* 55, no. 18 (2021): 2513-2555. https://doi.org/10.1177/0021998321990734

[2] Castanie, Bruno, Christophe Bouvet, and Malo Ginot. "Review of composite sandwich structure in aeronautic applications." *Composites Part C: Open Access* 1 (2020): 100004. https://doi.org/10.1016/j.jcomc.2020.100004

[3] Rejab, M. R. M., and W. J. Cantwell. "The mechanical behaviour of corrugated-core sandwich panels." *Composites Part B: Engineering* 47 (2013): 267-277. https://doi.org/10.1016/j.compositesb.2012.10.031

[4] Keey, Tony Tiew Chun, and M. Azuddin. "Influence of injection temperatures and fiberglass compositions on mechanical properties of polypropylene." In *IOP Conference Series: Materials Science and Engineering*, vol. 210, no. 1, p. 012080. IOP Publishing, 2017. https://doi.org/10.1088/1757-899X/210/1/012080

[5] Haldar, A. K., V. Managuli, R. Munshi, R. S. Agarwal, and Z. W. Guan. "Compressive behaviour of 3D printed sandwich structures based on corrugated core design." *Materials today communications* 26 (2021): 101725. https://doi.org/10.1016/j.mtcomm.2020.101725

[6] Li, Huimin, Lei Ge, Baosheng Liu, Haoran Su, Tianyi Feng, and Daining Fang. "An equivalent model for sandwich panel with double-directional trapezoidal corrugated core." *Journal of Sandwich Structures & Materials* 22, no. 7 (2020): 2445-2465. https://doi.org/10.1177/1099636219837884

[7] Imran, Ali, Shijie Qi, Pengcheng Shi, Muhammad Imran, Dong Liu, Yingdan Zhu, and Guilin Yang. "Effect of core corrugation angle on static compression of self-reinforced PP sandwich panels and bending energy absorption of sandwich beams." *Journal of Composite Materials* 55, no. 7 (2021): 897-914. https://doi.org/10.1177/0021998320960531

[8] Biagi, Russell, Jae Yong Lim, and Hilary Bart-Smith. "In-Plane Compression Response of Extruded Aluminum 6061-T6 Corrugated Core Sandwich Columns." *Journal of the American Ceramic Society* 94 (2011): s76-s84. https://doi.org/10.1111/j.1551-2916.2011.04601.x

[9] Le, Vinh Tung, Tailie Jin, and Nam Seo Goo. "Mechanical behaviors and fracture mechanisms of CFRP sandwich composite structures with bio-inspired thin-walled corrugated cores." *Aerospace Science and Technology* 126 (2022): 107599. https://doi.org/10.1016/j.ast.2022.107599

[10] Biswas, Sandhyarani, Basu Deo, Amar Patnaik, and Alok Satapathy. "Effect of fiber loading and orientation on mechanical and erosion wear behaviors of glass–epoxy composites." *Polymer composites* 32, no. 4 (2011): 665-674. https://doi.org/10.1002/pc.21082

[11] Yan, L. L., Bo Yu, Bin Han, C. Q. Chen, Q. C. Zhang, and T. J. Lu. "Compressive strength and energy absorption of sandwich panels with aluminum foam-filled corrugated cores." *Composites Science and Technology* 86 (2013): 142-148. https://doi.org/10.1016/j.compscitech.2013.07.011

[12] Chun, Zhang, Qi Chao, Yan Leilei, Zhao Yuliang, and Zhang Yunwei. "3D Effect of Sandwich Panels with Aluminum-Foam-Filled Corrugated Plates Under Out-of-Plane Compression." *RARE METAL MATERIALS AND ENGINEERING* 51, no. 1 (2022): 36-43.

[13] Zhu, Keyu, Xitao Zheng, Cong Zhang, Niu Chen, Yagang Han, Leilei Yan, and M. Quaresimin. "Compressive response and energy absorption of all-composite sandwich panels with channel cores." *Composite Structures* 289 (2022): 115461. https://doi.org/10.1016/j.compstruct.2022.115461

[14] Han, Bin, Lei L. Yan, Bo Yu, Qian C. Zhang, Chang Q. Chen, and Tian J. Lu. "Collapse mechanisms of metallic sandwich structures with aluminum foam-filled corrugated cores." *J. Mech. Mater. Struct* 9, no. 4 (2014): 397-425. https://doi.org/10.2140/jomms.2014.9.397

[15] Chen, Liming, Shiwei Peng, Jian Liu, Houchang Liu, Liliang Chen, Bing Du, Weiguo Li, and Daining Fang. "Compressive response of multi-layered thermoplastic composite corrugated sandwich panels: Modelling and experiments." *Composites Part B: Engineering* 189 (2020): 107899. https://doi.org/10.1016/j.compositesb.2020.107899

[16] Hou, Shujuan, Chengfu Shu, Shuyun Zhao, Tangying Liu, Xu Han, and Qing Li. "Experimental and numerical studies on multi-layered corrugated sandwich panels under crushing loading." *Composite Structures* 126 (2015): 371-385. https://doi.org/10.1016/j.compstruct.2015.02.039

[17] Ge, Lei, Huayong Zheng, Huimin Li, Baosheng Liu, Haoran Su, and Daining Fang. "Compression behavior of a novel sandwich structure with bi-directional corrugated core." *Thin-Walled Structures* 161 (2021): 107413. https://doi.org/10.1016/j.tws.2020.107413

[18] Rong, Yu, Jingxi Liu, Wei Luo, and Wentao He. "Effects of geometric configurations of corrugated cores on the local impact and planar compression of sandwich panels." *Composites Part B: Engineering* 152 (2018): 324-335. https://doi.org/10.1016/j.compositesb.2018.08.130

[19] He, Wentao, Linfeng Wang, Huancai Liu, Changzi Wang, Lu Yao, Qing Li, and Guangyong Sun. "On impact behavior of fiber metal laminate (FML) structures: A state-of-the-art review." *Thin-Walled Structures* 167 (2021): 108026. https://doi.org/10.1016/j.tws.2021.108026

[20] Gibson, Lorna J. "Cellular solids." *Mrs Bulletin* 28, no. 4 (2003): 270-274. doi: https://doi.org/10.1557/mrs2003.79. https://doi.org/10.1557/mrs2003.79